HHS Public Access

Author manuscript

Nanoscale. Author manuscript; available in PMC 2015 August 01.

Published in final edited form as:

Nanoscale. 2014 ; 6(3): 1567–1572. doi:10.1039/c3nr04804g.

Biodegradable Cationic Polymeric Nanocapsules for Overcoming Multidrug Resistance and Enabling Drug-Gene Co-Delivery to Cancer Cells

Chih-Kuang Chen[a,‡], **Wing-Cheung Law**[b,‡], **Ravikumar Aalinkeel**[c], **Yun Yu**[a], **Bindukumar Nair**[c], **Jincheng Wu**[a], **Supriya Mahajan**[c], **Jessica L. Reynolds**[c], **Yukun Li**[a], **Cheng Kee Lai**[a], **Emmanuel S. Tzanakakis**[a], **Stanley A. Schwartz**[c], **Paras N. Prasad**[b,d], and **Chong Cheng**[a]

Stanley A. Schwartz: sasimmun@buffalo.edu; Paras N. Prasad: pnprasad@buffalo.edu; Chong Cheng: ccheng8@buffalo.edu

[a]Department of Chemical and Biological Engineering, University at Buffalo, The State University of New York, Buffalo, NY 14260, USA

[b]Institute for Lasers, Photonics and Biophotonics, and Department of Chemistry, University at Buffalo, The State University of New York, Buffalo, NY 14260, USA

[c]Department of Medicine, Division of Allergy, Immunology, and Rheumatology, University at Buffalo, The State University of New York, Buffalo General Hospital, Buffalo, NY 14203, USA

[d]Department of Chemistry, Korea University, Seoul, 136-701, Korea

Abstract

Having unique architectural features, cationic polymeric nanocapasules (NCs) with well-defined covalently-stabilized biodegradable structures were generated as potentially universal and safe therapeutic nanocarriers. These NCs were synthesized from allyl-functionalized cationic polylactide (CPLA) by highly efficient UV-induced thiol-ene interfacial cross-linking in transparent miniemulsions. With tunable nanoscopic sizes, negligible cytotoxicity and remarkable degradability, they are able to encapsulate doxorubicin (Dox) with inner cavities and bind interleukin-8 (IL-8) small interfering RNA (siRNA) with cationic shells. The Dox-encapsulated NCs can effectively bypass P-glycoprotein (Pgp)-mediated multidrug resistance of MCF7/ADR cancer cells, thereby resulting in increased intracellular drug concentration and reduced cell viability. In vitro studies also showed that the NCs loaded with Dox, IL-8 siRNA and both agents can be readily taken up by PC3 prostate cancer cells, resulting in significant chemotherapeutic effect and/or IL-8 gene silencing.

Introduction

With cancer continuing to be one of the world's most devastating diseases, the development of nanomedicine approaches using novel carriers for cancer chemotherapy and gene therapy

Correspondence to: Stanley A. Schwartz, sasimmun@buffalo.edu; Paras N. Prasad, pnprasad@buffalo.edu; Chong Cheng, ccheng8@buffalo.edu.

‡These authors contributed equally.

†Electronic Supplementary Information (ESI) available: Experimental section; and Fig. S1–6. See DOI: 10.1039/b000000x/

has generated widespread interests.[1–7] Chemotherapy remains one of the primary forms of treatment for many cancers.[8] However, intrinsic and acquired multidrug resistance (MDR) by cancer cells is a major challenge in chemotherapy and contributes to most treatment failures for cancer patients.[9] Overexpression of transporter proteins, especially P-glycoprotein (Pgp), plays a key role in MDR through enhanced efflux of drugs.[10] Significant efforts have been made to develop Pgp inhibitors for reversing MDR, however most of these inhibitors exhibit relatively limited specificity and efficacy in clinic trials.[11–12] Moreover, the pharmacokinetic profile of anticancer drugs may also be altered by Pgp inhibitors, leading to systemic cytotoxicity and reduced therapeutic effects.[13] Therefore, the utilization of chemotherapeutic carriers to circumvent MDR has become an appealing alternative strategy to resolve MDR in the treatment of cancers.[14–17] Gene therapy has also been developed for cancer treatment,[18–19] requiring effective gene delivery to target cancer cells. Combination therapies using co-delivery of drugs and genes may produce synergistic effects and have become an emerging area of research.[20–26] With inner cavities available for loading therapeutics, nanocapsules (NCs) are an important class of therapeutic carriers.[27–29] However, their applications in bypassing MDR and enabling drug-gene co-delivery have not been reported.

Although a broad variety of therapeutic carriers with different sizes and structural features have been developed, we propose cross-linked biodegradable cationic polymer NCs (10–100 nm) as novel carriers with optimal structures for therapeutic delivery based on five major considerations. First, nanocarriers with sizes of 10–100 nm can avoid fast systemic clearance and capitalize on passive tumor targeting via their enhanced permeability and retention (EPR) effect.[30–32] Second, capsular carriers possess hollow structures with large relative surface area, and may be loaded with significant amounts of therapeutic agents via both encapsulation and surface adsorption.[33–34] Third, cationic shells of NCs can enable their surface binding of negatively-charged cargos (including genetic materials), and promote their cell uptake and water solubility.[35] Fourth, relative to assembled scaffolds, cross-linked carriers have critical structural stability.[36] Fifth, a polymer precursor with remarkable biodegradability and low cytotoxicity is used to construct the NCs, and therefore, their long term side effects can be minimized.[37] However, thoughtful synthetic design is required for the preparation of NCs with tailored structures. Specifically, although aliphatic polyesters are the major types of synthetic biodegradable polymers with broad biomedical applications, the preparation of aliphatic polyester-based cationic NCs is highly challenging.

Herein, we report unique nanoformulations using cationic polymeric NCs as carriers for therapeutic delivery. With inner cavities, these NCs can encapsulate chemotherapeutics to bypass Pgp-mediated efflux pump, thereby resulting in increased intracellular drug concentration. Because their cationic shells can bind genes via electrostatic adsorption, they can also be utilized in dual model therapy for delivery of both drugs and genes.

Results and Discussion

The NCs with targeted structural features were synthesized by highly efficient UV-induced thiol-ene interfacial cross-linking in transparent miniemuslions (Scheme 1).[38–39] With

insignificant cytotoxicity and verified ability to form nanocomplexes with genes, allyl-functionalized cationic polylactide (CPLA) was selected as the biodegradable, cationic, amphiphilic precursor for the NCs.[40–41] With 30 and 20 mol% of repeat units carrying allyl and tertiary amine-based cationic groups respectively, CPLA (DP_n^{NMR} = 80, M_n^{NMR} = 15.4 kDa, PDI^{GPC} = 1.17) was prepared by the method which we reported recently.[40] Alkyl 3-mercaptopropionate cross-linkers, such as 1,4-butanediol bis(3-mercapto-propionate), were selected ($[SH]_0/[allyl]_0$ = 1–1.05). 2,2'-Dimethoxy-2-phenylacetophenone (DMPA) was used as the photoinitiator. Due to the high surfactant efficiency of CPLA, transparent oil-in-water miniemulsions were obtained using only 3 wt% of CPLA relative to chloroform ($W_{water}/W_{chloroform}$ = 21), after 20 min of ultrasonication of the reaction mixtures. Subsequently, interfacial thiol-ene cross-linking induced by 30 min of UV irradiation (λ_{max} = 365 nm) yielded the NCs.

Well-controlled structures of the resulting NCs were verified. Quantitative reaction efficiency in each trial was revealed by ^{1}H NMR and FT-IR analyses, based upon the absence of the resonance of allyl C*H* proton at 5.78 ppm (Fig. 1a) and the C=C stretching vibration at 1640 cm^{-1} (Fig. S1).[38,40] Thiol-functionalized NCs were obtained when an excess amount of cross-linker ($[SH]_0/[allyl]_0$ = 1.05) was used. The preparation process was monitored by dynamic light scattering (DLS). The DLS data were reproducible, and the sizes of miniemulsion nanodroplets and the NCs can be tuned by altering the miniemulsification conditions. For instance, with a smaller energy input via ultrasonication, NCs **1** (volume-average hydrodynamic diameter ($D_{h,v}$) = 50 nm) obtained at a microtip amplitude of 40 μm were significantly larger than NCs **2** ($D_{h,v}$ = 24 nm) obtained at a microtip amplitude of 68 μm. For each trial, before the removal of chloroform, the nanodroplets and the NCs exhibited similar dimensions, indicating a well-controlled template synthesis (Fig. 1b and S2); after the removal of cholorform, the NCs showed reduced hydrodynamic sizes (NCs **1**: $D_{h,v}$ = 35 nm; NCs **2**: $D_{h,v}$ = 22 nm). TEM imaging of NCs confirmed their capsule-like morphology (Fig. 1c and S2). For instance, NCs **1** showed a capsule-like structure with surface dimensions around 50 nm which were comparable to their hydrodynamic sizes. Zeta potential measurements (NCs **1**: 54 mV; NCs **2**: 45 mV) verified the presence of positive charges on the cationic shells of NCs. Hydrolytic degradability of these NCs was probed by monitoring the variations of relative intensity of the scattered light (I/I_0) of their aqueous solution at physiological pH and 37 °C.[38] For instance, according to the I/I_o values, NCs **1** essentially degraded to smaller residues within 45 h (Fig. S3). Their considerable hydrolytic degradability may be ascribed to presence of high surface density of cationic groups and large relative surface area. The degradation of NCs would become slow at lower temperatures.[40] It should be noted that the degradation profile of NCs may not correlate directly with the release rate of encapsulated payloads. Particularly, small molecule caroges would be able to diffuse out from NCs through their polymeric shells before the breaking down of NCs.

A cell viability study was conducted to assess any cytotoxicity of CPLA NCs. Using the cell proliferation (MTS) assay (Fig. 2), these NCs showed no appreciable cytotoxicity towards two different cancer cell lines, including a multidrug-resistant breast cancer line (MCF7/ADR) and a prostate cancer cell line (PC3), at a dosage up to 360 μg/mL within 48 h of

incubation. Because of their remarkable degradability, their long term toxicity should also be minimal.[37]

Small molecule drugs and therapeutic genes can be readily loaded to the CPLA NCs by encapsulation through their cavities and electrostatic adsorption on their positively-charged surface, respectively (Scheme 1). By choosing doxorubicin (Dox),[42] one of the most commonly used chemotherapeutic agents, as the model drug, Dox-encapsulated CPLA-NCs (Dox-CPLA NCs; 11.6 wt% of Dox relative to CPLA; 74% encapsulation efficiency) were prepared via in situ encapsulation following the same conditions for the preparation of NCs **2**, except the addition of Dox (15.6 wt% relative to CPLA) before ultrasonication and the removal of free Dox from water phase via extraction after cross-linking. The resulting Dox-CPLA NCs ($D_{h,v}$ = 20.0 nm, ζ-potential = 42 mV) had hydrodynamic sizes slightly smaller than NCs **2**. On the other hand, because interleukin-8 (IL-8) small interfering RNA (siRNA) can silence gene overexpression of IL-8 proteins which has been verified as a significant tumor growth factor causing angiogenesis in cancer cells,[43–44] it was selected as the representative gene material for surface adsorption by CPLA NCs. IL-8 siRNA-loaded CPLA NCs (IL-8-siRNA-CPLA NCs) were readily obtained by mixing aqueous solutions of IL-8 siRNA and CPLA NCs **2**. Different weight ratios of NCs to siRNA (W_{NCs}/W_{siRNA} = 30, 65, 100 and 150) were used. The occurrence of adsorption of IL-8 siRNA on the shell surface of CPLA NCs was supported by the increased $D_{h,v}$ of IL-8-siRNA-CPLA NCs relative to the naked NCs **2** ($D_{h,v}$ = 22 nm). For instance, with W_{NCs}/W_{siRNA} of 30, the resulting IL-8-siRNA-CPLA NCs exhibited a $D_{h,v}$ of 28 nm. Electrophoresis gel retardation assay showed strong binding of siRNA with CPLA NCs (Fig. S4). Moreover, the CPLA NCs could be readily co-loaded with both small molecule drug and therapeutic gene. For instance, Dox/IL-8-siRNA-CPLA NCs carrying 11.6 wt% Dox and 3.3 wt% IL-8 siRNA relative to NCs were obtained by simply mixing aqueous solutions of IL-8 siRNA and Dox-CPLA NCs; such drug and gene loading levels were significant, although the preparation process was not optimized to maximize the loading.

We hypothesized that drug encapsulated by NCs can bypass the Pgp-mediated efflux pump, thereby resulting in increased intracellular drug concentration and enhanced therapeutic efficacy. Because Dox can be recognized and exported by Pgp from multidrug-resistant cancer cells and the MCF7/ADR cell line is a widely studied, stable MDR model with high expression of Pgp, in vitro studies were conducted using Dox-CPLA NCs and free Dox to treat MCF7/ADR cell line for the verification of the hypothesis.[11,16] Based on the fluorescence of Dox, the internalization of Dox ($[Dox]_0$ = 40 μM) in MCF7/ADR cells was visualized using confocal microscopy. Because the intracellular concentrations of free Dox were greatly affected by the efflux pump, the intracellular concentration of Dox was minimal at 4 and 8 h post treatment (Fig. 3a). In sharp contrast, robust Dox fluorescence was observed for the trials using Dox-CPLA NCs. Noticeably, the confocal images, which were selectively obtained from survival cells, did not reflect the total cell numbers of trials at different incubation times. The quantification of confocal images of intracellular Dox concentrations over time further revealed that Dox-CPLA NCs led to 3.6 fold and 3.2 fold enhanced concentrations of Dox in the cytoplasm at 4 and 8 h post treatment respectively, as compared with free Dox alone (Fig. 3b).

Flow cytometric analysis of intracellular amounts of Dox was further performed. After 4 h post treatment of MCF7/ADR cells ($[Dox]_0$ = 0.4 μM), relative to free Dox, Dox-CPLA NCs resulted in a 50% increase in Dox-positive cells (Fig. 3c and S5). The above results clearly demonstrate that the Pgp efflux pump can be successfully evaded through encapsulation of Dox into the NCs. The enhanced cell affinity via the positively charged surface of NCs might also contribute to the increased cellular uptake of the encapsulated Dox.

MTS assays on MCF7/ADR showed that the enhanced cellular uptake of Dox via CPLA NCs consequently led to higher anti-tumor efficacy. MCF7/ADR cells were treated with free Dox and Dox-CPLA NCs with various concentrations of Dox (0.2, 1, 4, 10, 20 and 40 μM) for 48 h. As compared with free Dox, Dox-CPLA NCs exhibited a significantly enhanced anti-proliferation effect (15–20% lower cell viability than free Dox) at all concentrations of Dox studied (Fig. 3d). On the other hand, control experiments using MCF7 cell line with the absence of overexpressed Pgp showed that Dox-CPLA NCs only resulted in a slightly or negligibly enhanced toxicity in MCF7 cells as compared with free Dox (Fig. 3e). The results further support that enhanced anti-tumor efficacy of Dox-CPLA NCs in the multidrug-resistant cells is due to evading the Pgp efflux pump by the NCs, thus facilitating intracellular delivery of Dox.

We also hypothesized that the CPLA NCs can serve as versatile nanocarriers to deliver both small molecule drugs and therapeutic genes into cancer cells. To examine the hypothesis, Dox was used as the model drug;[42] IL-8 siRNA was selected as the model genetic material;[43–44] and the PC3 prostate cancer line was used.[40,45] As control studies for the co-delivery of Dox and IL-8 siRNA, individual deliveries of these therapeutic agents into PC3 cells were investigated at first via Dox-CPLA NCs and IL-8-siRNA-CPLA NCs, respectively.

The delivery of Dox via CPLA NCs into PC3 cells was verified by confocal imaging of PC3 cells incubated with Dox-CPLA NCs ($[Dox]_0$ = 40 μM; Fig. 4a). A significant presence of Dox in the cells was observed after 8 h of incubation. Because PC3 cells are not multidrug-resistant, according to the MTS cell viability assay, Dox-CPLA NCs exhibited only slightly higher anti-tumor efficacies to PC3 cells than free Dox (Fig. 4b).

Although naked siRNA is susceptible to degradation and cannot effectively penetrate cell membrane,[40] successful delivery of IL-8 siRNA via CPLA NCs into the PC3 cells was verified by confocal imaging of the cells incubated with the CPLA NCs loaded with carboxyfluorescein (FAM)-labeled IL-8 siRNA ($[siRNA]_0$ = 0.1 μM; Fig. 4c). IL-8 siRNA carried by NCs accumulated around the cell membrane at 1 h of incubation, and then gradually internalized into the cytoplasm. Using various controls, the effect of IL-8-siRNA-CPLA NCs on gene silencing of IL-8 in the PC3 cells was investigated (Fig. 4d). Using the same concentration of siRNA (0.1 μM), greater suppression of IL-8 gene expression was achieved at a lower weight ratio of CPLA NCs to siRNA, suggesting an increase of the release rate of IL-8-siRNA was associated with the decrease of the weight ratio. Moreover, the gene silencing efficiency of IL-8 siRNA delivery *via* NCs with W_{NCs}/W_{siRNA} of 30 (WR-30; 41% knockdown) was comparable to that *via* commercial transfection agents,

including Mirus TransIT (MT; 39% knockdown) and lipofectamine (Lipo; 45% knockdown). It should be noted that free siRNA and scrambled siRNA transfected by MT exhibited no and negligible suppression of IL-8 gene expression (<10% knockdown) respectively.

Finally, co-delivery of Dox and IL-8 siRNA into PC3 cancer cells was probed through Dox/IL-8-siRNA^{FAM}-CPLA NCs (with 11.6 wt% Dox and 3.3 wt% IL-8 siRNA relative to NCs). After the incubation of PC3 cells with dually loaded NCs for 4 h, confocal images (Fig. 4e) clearly showed co-localization of fluorescence from both Dox and FAM-labeled siRNA in the same cells, confirming the utility of CPLA NCs as scaffolds for co-delivery of drug and gene. The therapeutic effect of Dox and IL-8 siRNA co-delivered *via* CPLA NCs was further studied at a constant siRNA concentration (0.1 μM).[22] Dox/IL-8-siRNA-CPLA NCs exhibited noticeably higher cyctotoxicity than Dox-CPLA NCs towards PC3 cells at low Dox concentrations (≤ 1 μM) presumably because the silencing of IL-8 gene (a tumor growth factor) made the treated cells more sensitive to Dox, although the enhancement of the therapeutic effect became less significant with the increase of Dox concentration (Fig. 4f).

Conclusions

In summary, we demonstrated a well-controlled synthesis of cationic polymeric NCs with cross-linked biodegradable structures, and their applications in encapsulation of drug to bypass MDR of MCF7/ADR cells and in the delivery of encapsulated drug and surface-adsorbed gene into PC3 cells. Such NCs may have broad applicability in effective individual as well as co-delivery of a broad variety of therapeutic agents into cancer cells, including multidrug-resistant cancer cells. These NCs hold much promise for subsequent in vivo, therapeutic applications (Fig. S6). Multifunctionalization of these NCs may provide combined therapeutic and diagnostic applications for a wide range of diseases besides cancer.[46–47]

Supplementary Material

Refer to Web version on PubMed Central for supplementary material.

Acknowledgements

This work was supported by grants from National Science Foundation CBET-1133737 and DMR-1206715 (C. Cheng), and the National Institute of Health R21-CA-167177-01A1(S. A. Schwartz), NIDA-1R21DA030108-01 (S. Mahajan), K01DA024577 (J. Reynolds) and R01-HL103709 (E. S. Tzanakakis), as well as the startup funding from University at Buffalo (C. Cheng).

Notes and references

1. Duncan R. Nat. Rev. Cancer. 2006; 6:688–701. [PubMed: 16900224]
2. Farokhzad OC, Cheng J, Teply BA, Sherifi I, Jon S, Kantoff PW, Richie JP, Langer R. Proc. Natl. Acad. Sci. U.S.A. 2006; 103:6315–6320. [PubMed: 16606824]
3. Riehemann K, Schneider SW, Luger TA, Godin B, Ferrari M, Fuchs H. Angew. Chem. Int. Ed. 2009; 48:872–897.
4. Fox ME, Szoka FC, Fréchet JMJ. Acc. Chem. Res. 2009; 42:1141–1151. [PubMed: 19555070]

5. Johnson JA, Lu Y-Y, Burts AO, Lim Y-H, Finn MG, Koberstein JT, Turro NJ, Tirrell DA, Grubbs RH. J. Am. Chem. Soc. 2011; 133:559–566. [PubMed: 21142161]
6. Cheetham AG, Zhang P, Lin Y-a, Lock LL, Cui H. J. Am. Chem. Soc. 2013; 135:2907–2910. [PubMed: 23379791]
7. Prasad, PN. Introduction to Nanomedicine and Nanobioengineering. Hoboken, New Jersey: Wiley; 2012.
8. Chabner BA, Roberts TG. Nat. Rev. Cancer. 2005; 5:65–72. [PubMed: 15630416]
9. Longley DB, Johnston PG. J. Pathol. 2005; 205:275–292. [PubMed: 15641020]
10. Bellamy WT. Annu. Rev. Pharmacol. Toxicol. 1996; 36:161–183. [PubMed: 8725386]
11. Szakacs G, Paterson JK, Ludwig JA, Booth-Genthe C, Gottesman MM. Nat. Rev. Drug Discov. 2006; 5:219–234. [PubMed: 16518375]
12. Fletcher JI, Haber M, Henderson MJ, Norris MD. Nat. Rev. Cancer. 2010; 10:147–156. [PubMed: 20075923]
13. Oza AM. Novartis Found Symp. 2002; 243:103–115. [PubMed: 11990771]
14. Jabr-Milane LS, van Vlerken LE, Yadav S, Amiji MM. Cancer Treat. Rev. 2008; 34:592–602. [PubMed: 18538481]
15. Yan Y, Ochs CJ, Such GK, Heath JK, Nice EC, Caruso F. Adv. Mater. 2010; 22:5398–5403. [PubMed: 20976679]
16. Lee Y, Graeser R, Kratz F, Geckeler KE. Adv. Funct. Mater. 2011; 21:4211–4218.
17. Wang F, Wang YC, Dou S, Xiong MH, Sun TM, Wang J. ACS Nano. 2011; 5:3679–3692. [PubMed: 21462992]
18. McCormick F. Nat. Rev. Cancer. 2001; 1:130–141. [PubMed: 11905804]
19. Pack DW, Hoffman AS, Pun S, Stayton PS. Nat. Rev. Drug Discov. 2005; 4:581–593. [PubMed: 16052241]
20. Creixell M, Peppas NA. Nano Today. 2012; 7:367–379.
21. Khan M, Ong ZY, Wiradharma N, Attia ABE, Yang Y-Y. Adv. Healthcare Mater. 2012; 1:373–392.
22. Wang Y, Gao S, Ye W-H, Yoon HS, Yang Y-Y. Nat Mater. 2006; 5:791–796. [PubMed: 16998471]
23. Garbuzenko OB, Saad M, Pozharov VP, Reuhl KR, Mainelis G, Minko T. Proc. Natl. Acad. Sci. U.S.A. 2010; 107:10737–10742. [PubMed: 20498076]
24. Wiradharma N, Tong YW, Yang Y-Y. Biomaterials. 2009; 30:3100–3109. [PubMed: 19342093]
25. Han L, Huang R, Li J, Liu S, Huang S, Jiang C. Biomaterials. 2011; 32:1242–1252. [PubMed: 20971503]
26. Torney F, Trewyn BG, Lin VS, Wang K. Nat. Nanotechnol. 2007; 2:295–300. [PubMed: 18654287]
27. Mora-Huertas CE, Fessi H, Elaissari A. Int. J. Pharm. 2010; 385:113–142. [PubMed: 19825408]
28. Landfester K, Musyanovych A, Mailaender V. J. Polym. Sci., Part A: Polym. Chem. 2010; 48:493–451.
29. Richardson JJ, Ejima H, Loercher SL, Liang K, Senn P, Cui J, Caruso F. Angew. Chem. Int. Ed. 2013; 52:6455–6458.
30. Bertrand N, Leroux J-C. J. Control Release. 2012; 161:152–163. [PubMed: 22001607]
31. Petros RA, DeSimone JM. Nat. Rev. Drug Discov. 2010; 9:615–627. [PubMed: 20616808]
32. Elsabahy M, Wooley KL. Chem. Soc. Rev. 2012; 41:2545–2561. [PubMed: 22334259]
33. De Cock LJ, De Koker S, De Geest BG, Grooten J, Vervaet C, Remon JP, Sukhorukov GB, Antipina MN. Angew. Chem., Int. Ed. 2010; 49:6954–6973.
34. Esser-Kahn AP, Odom SA, Sottos NR, White SR, Moore JS. Macromolecules. 2011; 44:5539–5553.
35. Zhang K, Fang H, Wang Z, Taylor J-SA, Wooley KL. Biomaterials. 2009; 30:968–977. [PubMed: 19038441]
36. O'Reilly RK, Hawker CJ, Wooley KL. Chem. Soc. Rev. 2006; 35:1068–1083. [PubMed: 17057836]

37. Pridgen EM, Langer R, Farokhzad OC. Nanomedicine. 2007; 2:669–680. [PubMed: 17976029]
38. Zou J, Hew CC, Themistou E, Li Y, Chen C-K, Alexandridis P, Cheng C. Adv. Mater. 2011; 23:4274–4277. [PubMed: 22039596]
39. Li Y, Themistou E, Das BP, Christian-Tabak L, Zou J, Tsianou M, Cheng C. Chem. Commun. 2011; 47:11697–11699.
40. Chen C-K, Law W-C, Aalinkeel R, Nair B, Kopwitthaya A, Mahajan SD, Reynolds JL, Zou J, Schwartz SA, Prasad PN, Cheng C. Adv. Healthcare Mater. 2012; 1:751–761.
41. Jones CH, Chen C-K, Jiang M, Fang L, Cheng C, Pfeifer BA. Mol. Pharmaceutics. 2013; 10:1138–1145.
42. Lasic DD. Nature. 1996; 380:561–562. [PubMed: 8606781]
43. Waugh DJJ, Wilson C. Clin. Cancer Res. 2008; 14:6735–6741. [PubMed: 18980965]
44. Aalinkeel R, Nair MP, Sufrin G, Mahajan SD, Chadha KC, Chawda RP, Schwartz SA. Cancer Res. 2004; 64:5311–5321. [PubMed: 15289337]
45. Eckman AM, Tsakalozou E, Kang NY, Ponta A, Bae Y. Pharm. Res. 2012; 29:1755–1767. [PubMed: 22322898]
46. Steichen SD, Caldorera-Moore M, Peppas NA. Eur. J. Pharm. Sci. 2013; 48:416–427. [PubMed: 23262059]
47. Fass L. Mol. Oncol. 2008; 2:115–152. [PubMed: 19383333]

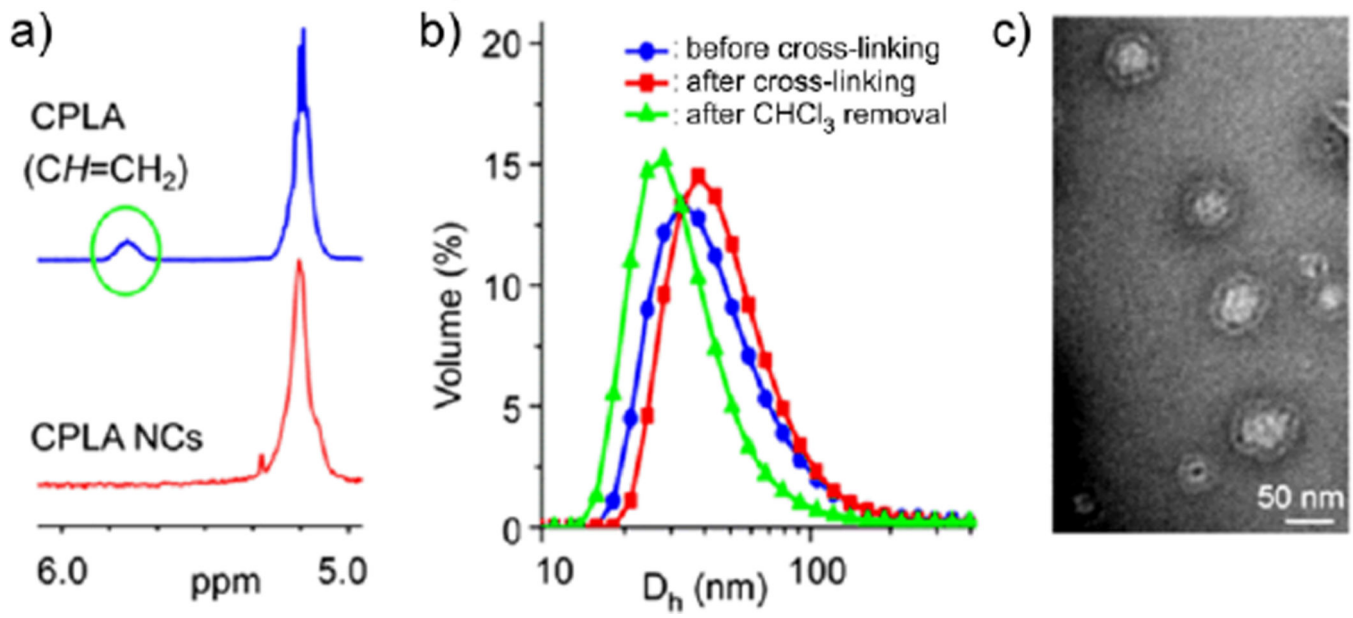

Fig. 1.

(a) Partial ^{1}H NMR spectra of CPLA and CPLA NCs **1**. (b) DLS results for the synthesis of CPLA NCs **1**. (c) TEM image of CPLA NCs **1**.

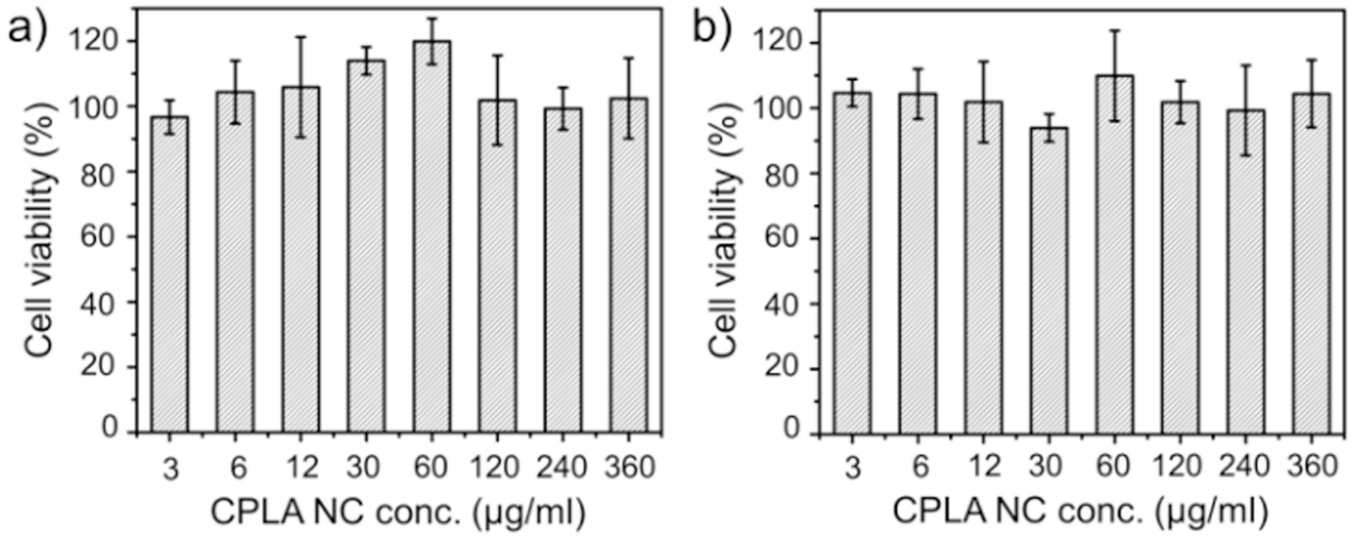

Fig. 2.

Cytotoxicity assessment of CPLA NCs **2** with 48 h of incubation: (a) MCF7/ADR cell line, and (b) PC3 cell line.

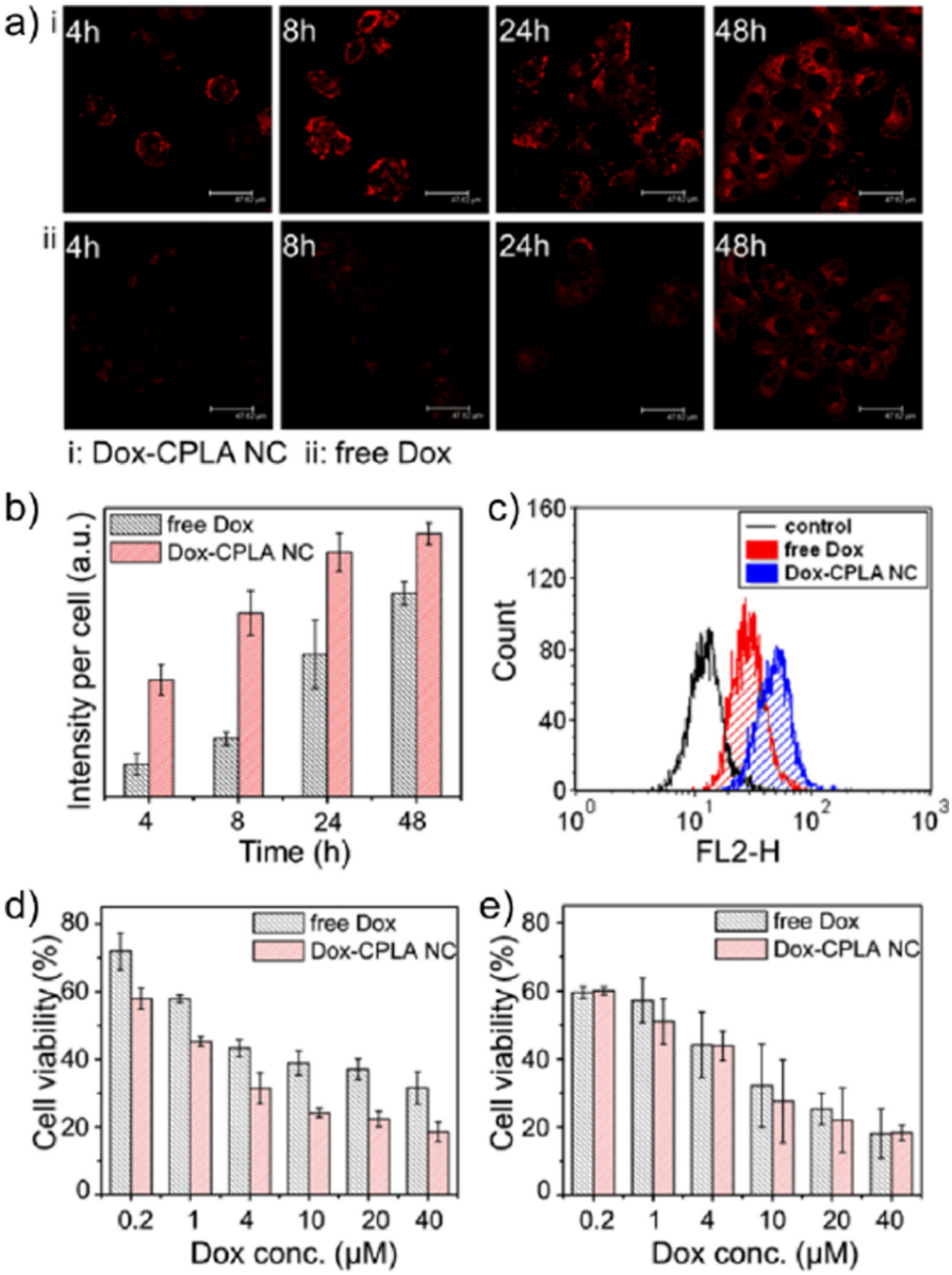

Fig. 3.

(a) Confocal images of MCF7/ADR cells incubated with free Dox and Dox-CPLA NCs ($[Dox]_0$ = 40 μM) for 4, 8, 24 and 48 h. (b) Fluorescence quantification of the confocal images using ImageJ software. (c) Flow cytometric histograms of intracellular Dox amounts in MDR7/ADR cells after 4 h of incubation with free Dox and Dox-CPLA NCs ($[Dox]_0$ = 0.4 μM; untreated MDR7/ADR cells was used as control). (d) Cytotoxicity assay of free Dox and Dox-CPLA NCs towards MCF7/ADR cells with 48 h of incubation. (e)

Cytotoxicity assay of free Dox and Dox-CPLA NCs towards MCF7 cells with 48 h of incubation.

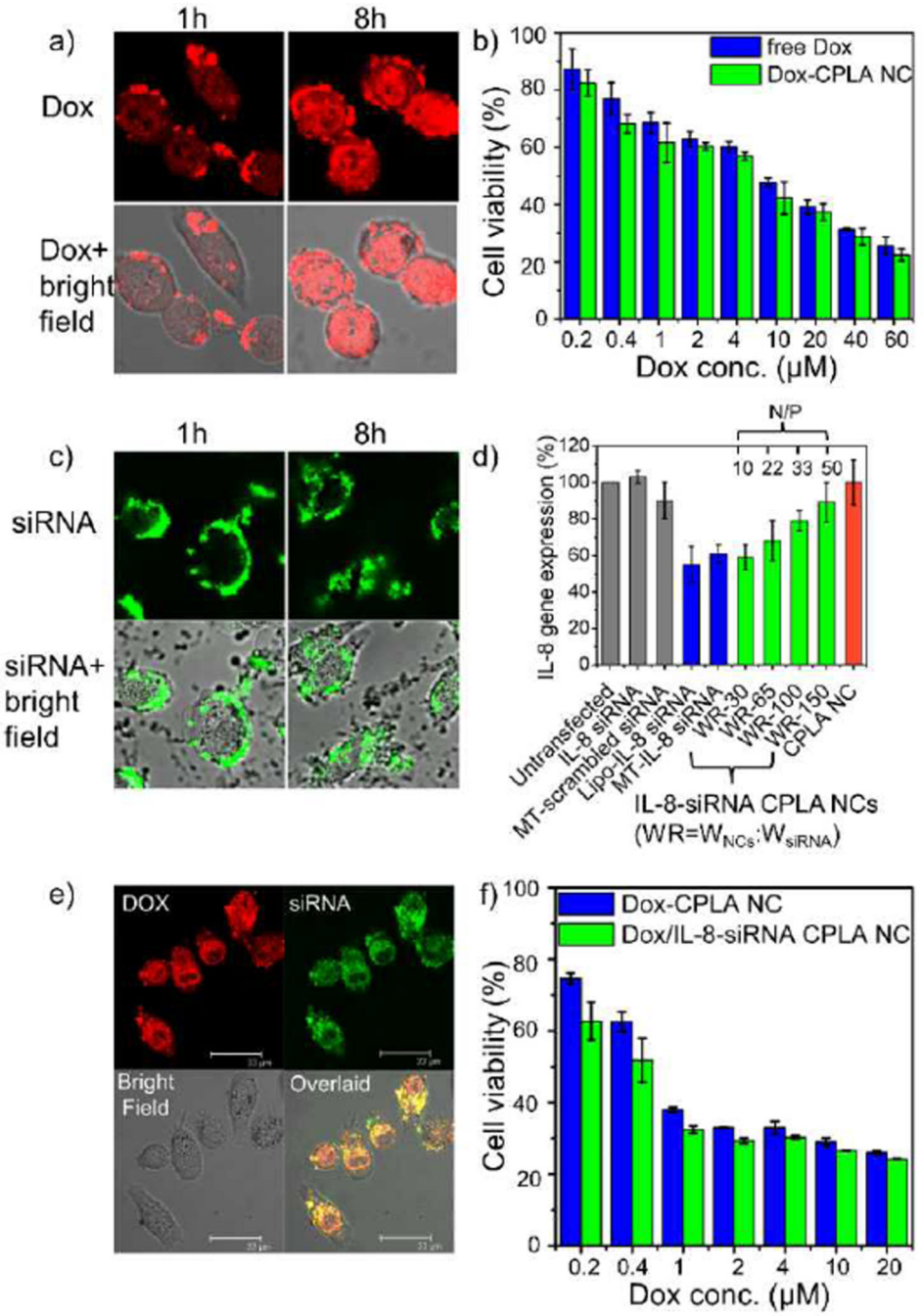

Fig. 4.

(a) Confocal images of PC3 cells treated with Dox-CPLA NCs for 1, 8 and 24 h. (b) Cell viability assay of PC3 cells treated with free Dox and Dox-CPLA NCs for 48 h. (c) Confocal images of PC3 cells treated with IL-8-siRNA^{FAM}-CPLA NCs (W_{NCs}: W_{siRNA} = 30) for 1, 8 and 24 h. (d) Transfection effects of IL-8-siRNA-CPLA NCs on IL-8 gene expression of PC3 cells. (e) Confocal images of PC3 cells treated with Dox/IL-8-siRNA^{FAM}-CPLA NCs for 4 h. (f) Cell viability assay of PC3 cells treated with Dox-CPLA NCs and Dox/IL-8-siRNA CPLA NCs ([siRNA] = 0.1 μM; W_{Dox}/W_{NCs} = 0.116) for 72 h.

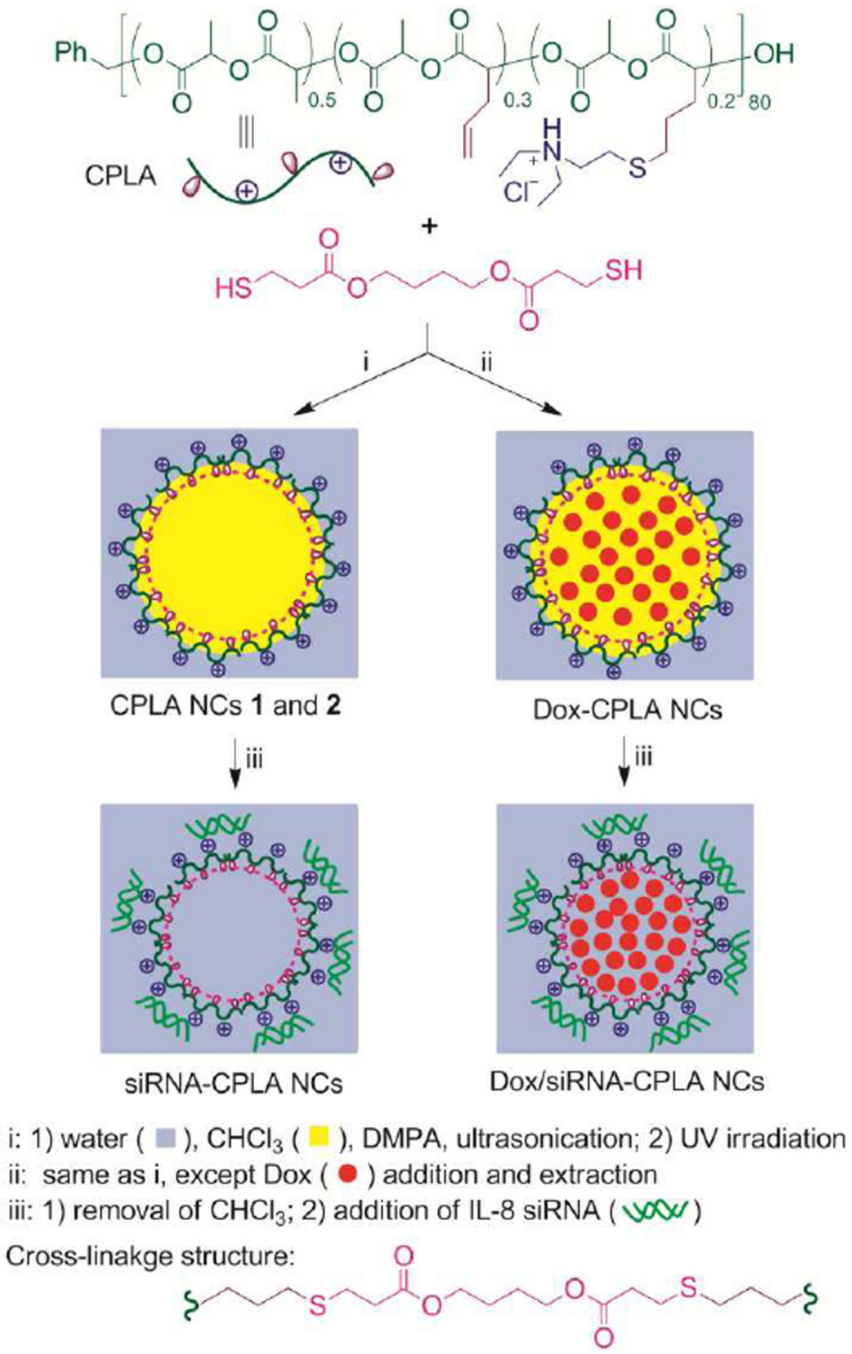

Scheme 1.
Synthesis of CPLA NCs and loading the NCs with therapeutic agents.